Hindawi
Journal of Chemistry
Volume 2020, Article ID 7234218, 12 pages
https://doi.org/10.1155/2020/7234218

Research Article

Removal of Textile Dyes by Chemically Treated Sawdust of Acacia: Kinetic and Equilibrium Studies

Hanane Tounsadi,[1] **Yousra Metarfi**,[1] **Noureddine Barka**,[2] **Mustapha Taleb**,[1] **and Zakia Rais**[1]

[1]*Laboratoire d'ingénierie d'Electrochimie de Modélisation et d'Environnement. Faculté des Sciences Dhar EL Mahraz, Université Sidi Mohamed Ben Abdallah, Fès, Morocco*
[2]*Sultan Moulay Slimane University, Research Group in Environmental Sciences and Applied Materials (SEMA), FP Khouribga B.P. 145, 25000 Khouribga, Morocco*

Correspondence should be addressed to Hanane Tounsadi; hananetounsadi@gmail.com

Received 22 January 2020; Revised 23 March 2020; Accepted 30 March 2020; Published 15 May 2020

Academic Editor: José Morillo

Sawdust of acacia tree has been successfully used to remove textile dyes from wastewater due to its good sorption properties and its good chemical stability. Two materials are prepared by chemical treatment, including acidic and basic sawdust of acacia. The biosorption tests were carried out on two synthetic dyes of textile which are methylene blue (MB) and brilliant blue (BB). Efficient removal of the both dyes has been achieved by the basic treated sawdust acacia. The modeling of biosorption kinetic shows that the biosorption of MB and that of BB are well described by the pseudo-first-order model for both the chemically treated biosorbents. Equilibrium data have also established using Langmuir and Freundlich isotherm models. Langmuir biosorption capacities are 8.13 and 267.04 mg/g onto basic sawdust acacia and 6.19 and 230.76 mg/g onto acidic sawdust acacia, respectively, for BB and MB sorption. A real final effluent of a textile industry was treated by sorption on both biosorbent basis of sawdust acacia. In fact, the kinetic sorption was rapid with a mass ratio of 1 g/L. However, the biosorption process combined with a biological treatment provides a better result through the physicochemical characteristics of the studied effluent.

1. Introduction

The progress of technology and the increase of textile industrial activities have increased the discharge of dyes in the wastewater. These toxic matters cause several damages to ecosystems due to their accumulation in the environment. Every year, more than 400,000 tons of reactive dyes are used to dye cellulosic fibers, mainly cotton [1]. Moreover, dyeing 1 kg of cotton could generate 200 kg of wastewater containing up to 50% of the initial input of dyes in the dye bath and up to 100 g/L of salts [2–4]. On the other hand, because most of the dyes used in industrial activities are synthetic, their degradation required a long period of time [5,6]. Due to their carcinogenic effect on biological systems, textile dyes caused a serious environmental problem worldwide [7]. Therefore, the effective removal of these hazardous dyes from industrial wastewater is the most challenge for improving the quality of aquatic ecosystems.

Numerous technologies have been developed to treat the dyeing aqueous media, including chemical precipitation [8], ultrafiltration [9], aerobic and anaerobic microbial degradation [10], electrocoagulation/flotation [11], advanced oxidation processes [12], electrochemical treatments [13], reverse osmosis [14], and adsorption [15] whereas most of these methods have proven their effectiveness in the removal of dyes. However, they have limited industrial applications because they are expensive, required high energy consumption and operation time, and in some cases can generate large quantities of secondary sludge, which must be also properly treated in order to prevent the environmental contamination [16]. Therefore, adsorption has long been recognized as a simple and economical process for the removal of textile dyes. Due to its efficiency, high selectivity, low cost, ease of operation, simplicity, and availability of low-cost adsorbents, adsorption could be considered a promising alternative for removing dyes from aqueous

solution. In the past decades, adsorption properties of persistent organic compounds by numerous materials have been reported [17]. However, readily available adsorbent materials such as clays, graphite, double hydroxide lamellar, resin, zeolite and mesoporous silica, activated carbon, and biosorbents have large adsorption capacity and good selectivity for various pollutants. Because of their low cost and availability, biosorbents are considered as alternative materials for environmental remediation. Several biomass-derived adsorbents have been examined for the removal of dyes including *Diplotaxis harra* and *Glebionis coronaria. L* [18], pectin-*Chlorella vulgaris* [19], grape pomace [20], banana peel [21], *Salvia hispanica* [22], peach gum [23], *Phragmites australis* [24], *Pseudomonas aeruginosa* [25], *Spirulina maxima*, and *Chlorella pyrenoidosa algae* [26].

The present work involves the removal of two dyes from aqueous solution by adsorption process using chemically treated sawdust of acacia tree with HCl or NaOH. In fact, the efficacity of the biosorbents has been extensively investigated by studying the effect of time, dosage quantity, and the equilibrium data. Further, biosorbents were characterized by point of zero charge, FTIR, SEM, and XRD. Also, the surface area of the studied biosorbents was determined using the methylene blue dye. Therefore, the final effluent discharge of an industrial effluent was treated by adsorption process using chemically treated sawdust of acacia with HCl or NaOH. In fact, the determination of the polluting load using biosorbents has been extensively investigated by studying the effect of time and dosage quantity.

2. Experimental Methods

2.1. Reagent Materials. All the chemicals used in this study were of analytical grade. Methylene blue (96%) and brilliant blue (BB) (96%), NaOH (89%), HNO_3 (69%), and NaCl (99%) were purchased from Sigma-Aldrich (Germany). The chemical structures and physical properties of these dyes are presented in Table 1.

2.2. Preparation of Biosorbents. The acacia tree used in this work is supplied from the Azrou region in Morocco. The cutting branches of the acacia are thoroughly washed with the water to remove adherent impurities, and then, they are crushed and sieved to small particles with size ranging from 50 to 500 μm. The final powder has a sweet corn color. 20 g of the acacia powder was chemically treated with 200 ml of NaOH (1M) or HCl (1M) for 3 h. Both residual products are washed several times to remove traces of NaOH and HCl. Afterwards, they are dried in an oven at 80°C for 24 h. Finally, two biosorbents based on acacia are obtained, which are A-NaOH and A-HCl.

2.3. Characterization of Biosorbents

2.3.1. Point of Zero Charge (pH_{PZC}). The point of zero charge (pH_{PZC}) was determined by the pH drift method according to the method proposed by Noh and Schwarz [27]. The pH of NaCl aqueous solution (50 ml at 0.01 mol/L) was adjusted to successive initial values in the range of 2.0 and 12.0 by the addition of HNO_3 (0.1 N) and/or NaOH (0.1 N). More there, 0.05 g of each carbon was added to the solution and stirred for 6 h. The final pH was measured and plotted versus the initial pH. The pH_{PZC} was determined at the value for which $pH_{final} = pH_{initial}$.

2.3.2. Infrared Spectroscopy. Infrared absorption spectroscopy spectra of biosorbents were illustrated at room temperature on a Fourier transform infrared spectroscopy (VERTEX 70). Before analysis, a small amount of powdered sample was dispersed in a matrix of KBr using weight ratio of carbon/KBr = 1/100 and then pressed to form transparent pellet. KBr was previously oven-dried to avoid interferences due to the presence of water, and FTIR spectrum was recorded at room temperature in the wavenumber range of 4000–400 cm^{-1}.

2.3.3. Scanning Electron Microscopy (SEM). The morphological characteristics of the prepared activated carbon were analyzed by scanning electron microscopy using a FEI Quanta 200 model. Small amount of each sample was finely powdered and mounted directly onto an aluminum sample holder using two-sided adhesive carbon model.

2.3.4. Development of Surface Area. The determination of the specific surface area of solids using methylene blue adsorption has been widely applied to activated carbons and also to clays [28]. Since the adsorption process of methylene blue was well described by the Langmuir models, the adsorption capacity (for complete monolayer coverage) can be used to evaluate the available area for mesopores. To have maximum sorption capacities of methylene blue, the adsorption isotherms were investigated. Stock solution of methylene blue was prepared by dissolving the desired weight of MB in distilled water. Sorption experiments were conducted in a series of beakers containing 100 mL of dye solution and 100 mg of each activated carbon. The mixtures were agitated for 12 h at room temperature. Equilibrium was established for methylene blue concentration between 20 and 500 mg/L. After each sorption experiment, samples were filtrated. The residual concentrations were determined by spectrophotometric method at the maximum absorbance wavelength of 665 nm.

The area occupied by an adsorbed methylene blue molecule is assumed to be 130 $Å^2$ as it is frequently cited in the literature [29]. The following formula was used to compute this specific surface area (S_g):

$$\mathbf{S_{sp}} = \mathbf{Q_m}.\mathbf{10^{-3}} \times \mathrm{N} \times \frac{\mathbf{A}}{\mathbf{M_{BM}}}, \quad (1)$$

where S_{sp} is the specific surface area of an adsorbent material, Q_m is the maximum adsorption capacity at equilibrium, N is the number of Avogadro ($N = 6.023.10^{23}$ atoms), A is the specific surface area of a molecule of methylene blue ($A = 130$ Å), and M_{BM} is the molar mass of methylene blue ($M_{BM} = 373.91\ gmol^{-1}$).

Table 1: Chemical and physical properties of methylene blue and brilliant blue.

Dye	Molecular weight (g/mol)	λ_{max} (nm)	Structure
Methylene blue (MB)	319.85	625	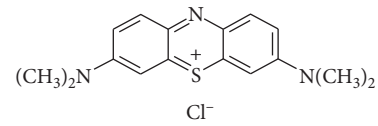
Brilliant blue (BB)	792.85	660	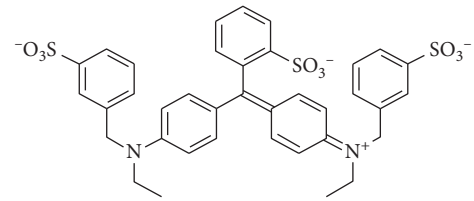

2.3.5. X-Ray Diffraction (XRD). Crystallographic characterization of the studied materials was examined by XRD measurements. The patterns were recorded in 2θ range from 10 to 70° using a Bruker-axs D2-phaser advance diffractometer operating at 30 kV and 10 mA with CuKα. The interlayer spacing d_{002} was determined using the Bragg equation:

$$d = \frac{\lambda}{2}\sin\theta, \tag{2}$$

where λ is the X-ray length and θ is the scattering angle for the peak position.

2.4. Experimental Studies

2.4.1. Biosorption of Synthetic Solution Dyes. Stock solutions of dyes were prepared by dissolving the desired weight of each dye in distilled water, and necessary concentrations were obtained by dilution. Sorption experiments were performed as follows: contact time from 0 to 360 min with 1 g/L of biosorbent and 10 mg/L of each solution dyes. Biosorbent dosage ranges from 0.5 to 10 g/L in a series of 50 mL beakers at the desired concentration, and initial concentration of dyes ranges from 1 to 10 mg/L for BB and from 10 to 500 mg/g for MB. These experiments were carried out at constant agitation in fixed pH of solution.

After completion of each adsorption experiment, the solid phase was separated from the liquid phase by filtration for 10 min. If necessary, sample was diluted by distilled water and the residual concentration was determined from its UV-Vis absorbance characteristic with the calibration curve method at the wavelength of maximum absorption of each dye. A UV-Vis with double beam spectrophotometer was used.

The adsorption capacity and adsorption yield were calculated using the following equations:

$$\mathbf{q_e} = \frac{(\mathbf{C_0} - \mathbf{C})}{\mathbf{R}}, \tag{3}$$

$$\%\text{removal} = \frac{(C_0 - C)}{C_0} * 100, \tag{4}$$

where q_e is the adsorbed quantity (mg/g), C_0 is the initial dye concentration (mg/L), C is the dye concentration at a time t (mg/L), and R is the mass adsorbents per liter of solution (g/l).

2.4.2. Biosorption Treatment of an Industrial Effluent. Final discharge of an industrial effluent from Sidi Brahim industry in Fez city was considered the "sampling site". The sampling was carried out by the composite method to know the variations of the pollution characteristics during a day. Three samples were taken, and each sample is a mixture of six separate samples for each hour, of equal volumes. At the end of the day, a calculation makes it possible to constitute a composite sample by the association of 6 samples. Therefore, three samples were taken for the reproducibility of the results.

The water samples were collected using sterile vials during the spring season of 2018. Then, they were stored in a cooler at 4°C during transport to the laboratory and then analyzed after 24 hours. Water temperature, electrical conductivity, and pH were measured in situ. The water samples and their methods of analysis are those recommended by AFNOR and enacted by Rodier [30]. Samples were analyzed by several physicochemical analyses including pH, conductivity, temperature, chemical oxygen demand (COD), biological oxygen demand (BOD_5), NTK, suspended matter (MES), and heavy metals (ML) (Cd, Cr, Cu, Ni, and Zn). The heavy metals were analyzed by inductively coupled plasma spectrometry (ICP AES) (Ultima 2_jobin yvon).

In the adsorption process of real effluent on A-NaOH and A-HCl, the adsorption kinetics and the effect of the mass of the both biosorbents are studied. Sorption experiments were performed as follows: contact time was applied from 0 to 360 min and biosorbent dosage was from 0.5 to 4 g/L in a series of 50 mL beakers.

These experiments were carried out at constant agitation in a fixed pH of the solution. The adsorption capacity and adsorption yield were calculated using the same process adopted in synthetic dye biosorption.

3. Result and Discussion

3.1. Characterization of Biosorbents

3.1.1. Point of Zero Charge (pH_{PZC}). Figure 1 illustrates the final pH change as a function of the initial pH used in the method of determining pH_{PCN} for both adsorbents: A-HCl and A-NaOH.

The figure shows that the final pH of the solution increases with the increase of the initial pH. This can be explained by the consumption of H^+ ions introduced into the solution by the surface of the solid. From the initial pH 5 and up to a pH of 10, the curves become parallel to the abscissa axis, i.e., the final pH of the solution is stable. Indeed, all H^+ ions introduced into solution are consumed by the surface of the solid until saturation of the sites. An increase in the final pH of the solution is observed from the initial pH of 10. This part corresponds to the saturation of the surface by the OH- ions, and all the introduced OH ions then remain in the solution.

The pH_{PCN} values are estimated at 2.5 and 6.3 for A-HCl and A-NaOH, respectively. This result indicates that the both biosorbents acquire a positive charge below these values, and above these values, they have negatively charged sites.

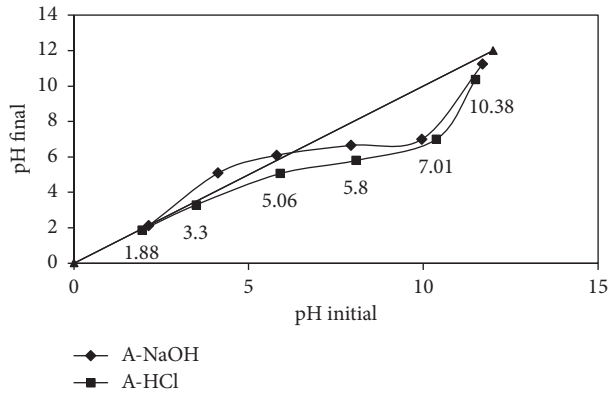

Figure 1: Point of zero charge acacia sawdust A-HCl and A-NaOH.

3.1.2. Infrared Spectroscopy. Infrared spectroscopy analysis of the chemically treated and raw acacia sawdust is shown in Figure 2. The spectrum of biosorbents basis acacia shows a band around 3336.54 cm^{-1} signifying the presence of OH hydroxyl groups of cellulose, lignins, and hemicellulose main components of wood. The bands at 2902.5 cm^{-1} correspond to C–H functions. The bands at 1266.45 are attributed to C–O functions. The bands at 1023.19 cm^{-1} can be corresponding to C–O–C functions. The bands appearing at the frequency between 720 and 400 cm^{-1} are characteristic of the C–H group in cellulose [31]. It could be seen that treated and untreated sawdust acacia present approximately the same bands with different intensities.

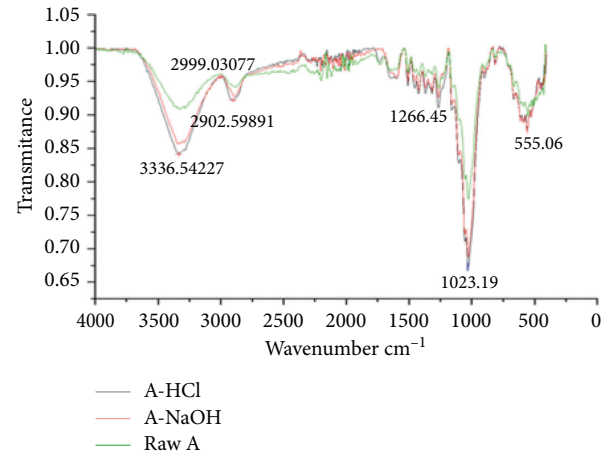

Figure 2: FTIR spectrum of raw-A, A-HCl, and A-NaOH biosorbents.

3.1.3. Development of Surface Area. The calculated values of biosorbents surface area are 698.91 m^2/g for A-NaOH and 523.51 m^2/g for A-HCl. In fact, the NaOH promotes a large surface area for sawdust acacia compared to the HCl. This result suggests different adsorption capacities between the both biosorbents.

3.1.4. Scanning Electron Microscopy (SEM). Scanning electron microscopy images of raw and treated sawdust of acacia are shown in Figure 3. This analysis indicates a significant difference in the surface morphology of the three materials. It can be seen that there are many pores in raw sawdust acacia corresponding to the cellulose microfibrils concentrated inside the fiber. After the treatment process, new pores of different sizes and cavities are formed due to the reaction between the raw material and the treatment agent. The external walls of the acacia fiber are composed mainly of hemicelluloses and the interfiber joining lamellae are composed of lignin. The latter joins the wood fibers together; the hemicelluloses bind the cellulose and the lignins.

3.1.5. X-Ray Diffraction (XRD). The X-ray diffractogram of acacia sawdust is difficult to interpret and shows the existence of a small quantity of crystals. The component of the wood that crystallizes is cellulose and is organized into a crystalline lattice by different ways.

The X-ray diffraction curves of the three samples of raw and chemically treated acacia sawdust are shown in Figure 4. The diffraction intensity increased after modification of the acacia sawdust. These results reveal an increase in the crystallinity index following the chemical treatment applied to sawdust, which are due to the improvement in the order of crystallites. The degree of crystallinity of the cellulose is higher in the treated samples than in the raw sawdust, due to the reduction of hemicelluloses during chemical treatment. However, the chemical treatment of acacia sawdust with HCl has an effect on increasing the crystallinity of the material, which is higher than that of acacia sawdust treated by NaOH. These observations are consistent with those of Alemdar et al. who made similar studies [31] on untreated and chemically treated Scots pine sawdust.

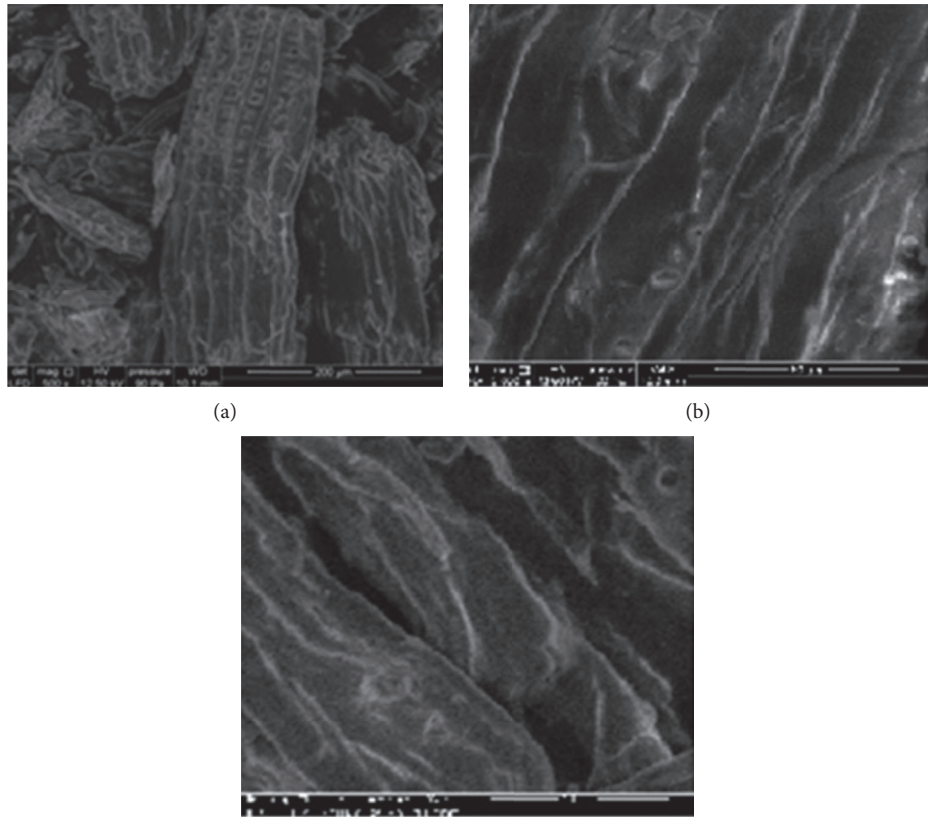

Figure 3: SEM images: (a) raw-A, (b) A-HCl, and (c) A-NaOH.

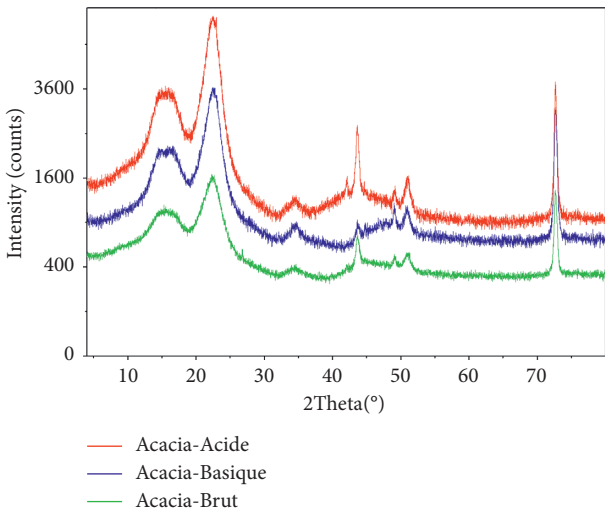

Figure 4: DRX diagram of raw acacia, A-HCl, and A-NaOH.

3.2. Biosorption Studies of Synthetic Dyes

3.2.1. Kinetic Biosorption. The sorption kinetic describes the rate of the reaction making it possible to determine the contact time involved in order to reach the equilibrium of the reaction. The kinetic sorption of the both dyes onto A-HCl and A-NaOH is presented in Figure 5. It could be seen that the biosorption process of brilliant blue is rapid; the equilibrium is reached after 40 min for A-NaOH and also for A-HCl. This moment is considered optimal for the removal of 7.789 mg/g and 6.758 mg/g of BB, respectively, on A-NaOH and on A-HCl. As for the methylene blue dye, the optimal time was reached up to 90 min for A-NaOH and A-HCl corresponding to a maximum capacity of 223.78 mg/g and 209.46 mg/g, respectively. Therefore, the biosorption efficiencies of chemically treated acacia sawdust are greater for methylene blue than for brilliant blue. However, it was seen that NaOH-treated sawdust exhibits a high adsorption capacity than that one treated by HCl.

The kinetic biosorption was initially fast for both dyes, which may be justified by the availability of active sites on the surface of the biosorbents. Then, it becomes slower until it reaches equilibrium. This can be due to the reduction of the contact surface after occupation of the majority of the active sites by each dye, which allows the creation of a competition with the remaining ions in solution.

In order to characterize the sorption efficiency of BB and MB onto the both sorbents, two kinetic models are used including the pseudo-first-order and the pseudo-second-order kinetic models.

The pseudo-first-order rate of Lagergren is based on solid capacity. This model considers the rate of occupation of sorption sites to be proportional to the number of unoccupied sites. It is one of the most widely used models for the sorption of a solute from liquid solution. It is generally represented as follows [32]:

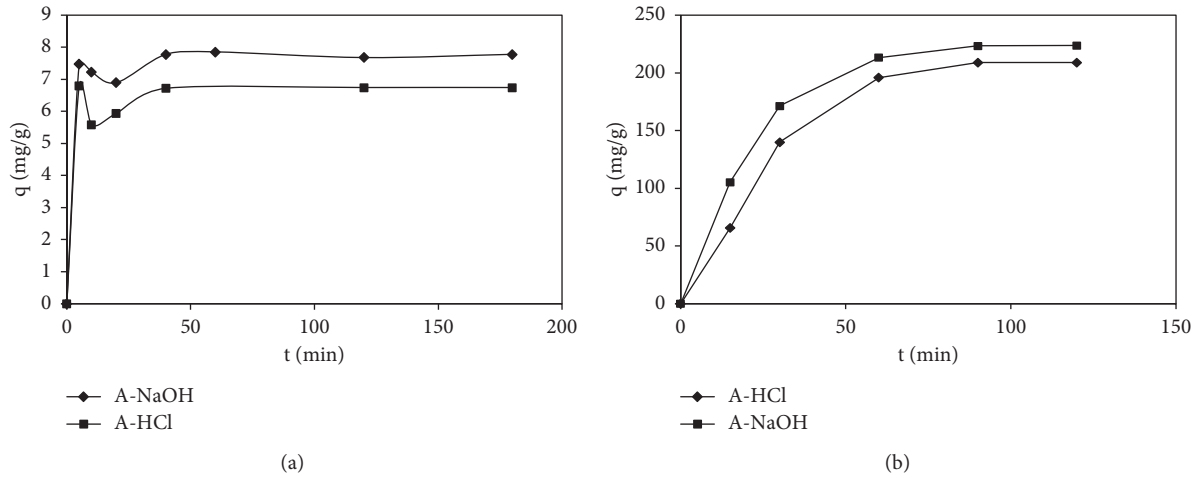

Figure 5: Biosorption kinetic of BB adsorption (a) and MB adsorption (b) onto A-NaOH and A-HCl. C_0(BB) = 10 mg/L, C_0(MB) = 100 mg/L, R = 0,5 g/L, and T = 25°C.

$$q = q_e\left(1 - e^{-k_1 t}\right), \tag{6}$$

where q_e and q (both in mg/g) are, respectively, the amounts of metal sorbed at equilibrium and at any time t (min) and k_1 (1/min) is the rate constant of sorption.

The pseudo-second-order model proposed by Ho and McKay [33] is based on the assumption that the sorption follows second-order chemisorption. The pseudo-second-order model may be expressed as follows:

$$q = \frac{k_2 q_e^2 t}{1 + k_2 q_e t}, \tag{7}$$

where k_2 (g/mg.min) is the rate constant of pseudo-second-order sorption.

The kinetic model fitting curves and the comparison of experimental and calculated sorption capacity (q) values can be used to establish the adapted kinetic models. Also, the obtained correlation coefficient (r^2) is considered a main factor to determine the adequate kinetic models and describe the sorption kinetics.

The parameters of the pseudo-first-order and pseudo-second-order kinetic models are calculated with the aid of the nonlinear regression. The obtained data are presented in Table 2. From these results, the correlation coefficients of the pseudo-first-order model obtained for BB and MB biosorption are higher than those ones of the pseudo-second-order model. The theoretical q_e biosorption capacities gave acceptable values when compared to the experimental ones for the both dyes in the pseudo-first-order model. Thus, the reaction involved in the present biosorption process is suitable to pseudo-first-order kinetic model. As a result, this model can describe very well the sorption process of the BB and MB onto the both biosorbents. It could be concluded that the removal of these dyes by studied biosorbents may be done with a physical sorption.

3.2.2. Influence of Biosorbent Dose. The variation of the percentage removal of BB and MB in function of the mass of the both biosorbents is presented in Figure 6. This figure shows that the biosorption reaction in a static reactor is very rapid by a strong discoloration by the both biosorbents. A mass ratio of 0.5 g/L for A-NaOH and A-HCl is considered optimal with a higher percentage of removal of BB and MB. Therefore, it can be seen that the increase of the biosorption yields of brilliant blue and methylene blue is not seemed to be affected by the increase in the mass of acacia sawdust. This could be attributed to a partial aggregation of the biosorbent which reduces the effective surface area for the biosorption.

3.2.3. Isotherm Sorption. Figure 7 shows the isotherm sorption of brilliant blue and methylene blue onto A-HCl and A-NaOH. It is clear that the biosorbed amount of the dye increases with increase of equilibrium concentration. The plots of the both studied isotherms indicate the type (L) form for the acacia sawdust treated with NaOH for the both synthetic dyes, and this type presents at a low concentration of the biosorbent in solution a downward concavity which reflects a decrease of free sites as the biosorption progresses. On the other hand, the biosorption of the both dyes onto acacia treated with HCl denotes an isotherm of the type (S) form. The description of the sorption isotherms is carried out by the application of Langmuir and Freundlich models:

(1) Langmuir Model. The Langmuir isotherm model assumes that sorption comes from the monolayer coverage of adsorbate over a homogeneous adsorbent surface [34]. This model supposes that sorption occurs on specific homogeneous sites within the adsorbent and all its sorption sites are energetically identical. The Langmuir isotherm can be written in the following form:

$$q_e = \frac{q_m * K_L * C_e}{1 + \left(K_L * C_e\right)}, \tag{8}$$

where q_m (mg/g) is the maximum monolayer biosorption capacity and K_L (L/mg) is the Langmuir equilibrium

Table 2: Pseudo-first-order and pseudo-second-order kinetic parameters for the sorption of BB and MB onto A-NaOH and A-HCl.

Dye	Biosorbent	q_{exp} (mg/g)	Pseudo-first-order			Pseudo-second-order		
			q_e (mg/g)	k_1 (1/min)	r^2	q_e (mg/g)	k_2 (g/mg min)	r^2
BB	A-NaOH	7.789	7.705	0.329	0.989	7.592	0.607	0.987
	A-HCl	6.758	6.436	8.955	0.964	6.491	1.158	0.963
MB	A-NaOH	223.46	227.38	0.044	0.998	187.43	−1.008	0.740
	A-HCl	209.00	221.77	0.030	0.999	163.92	1.194	0.988

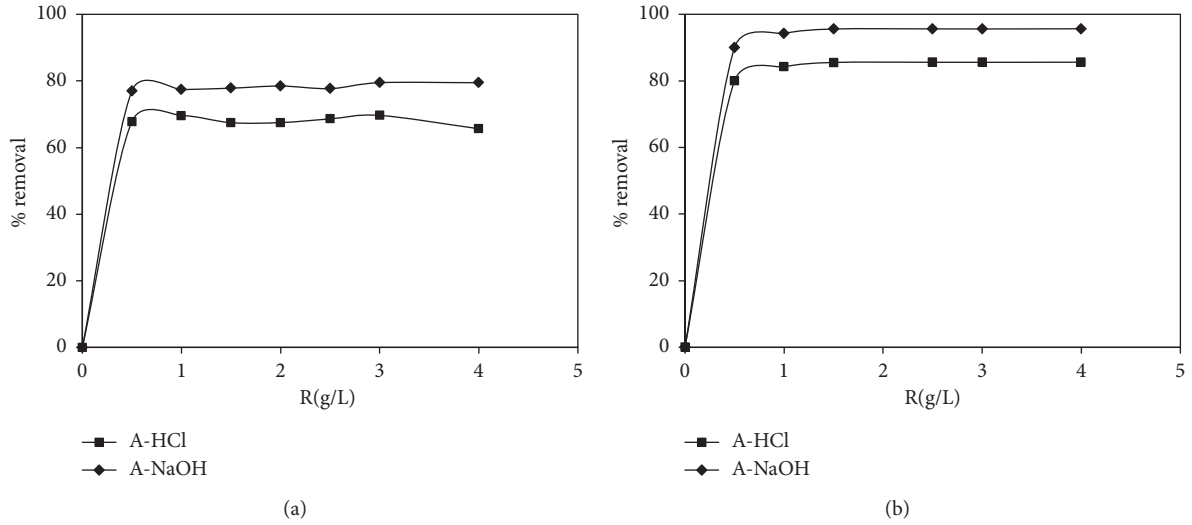

Figure 6: Percentage removal of BB (a) and MB (b) as a function of the mass of treated acacia sawdust: A-NaOH and A-HCl.

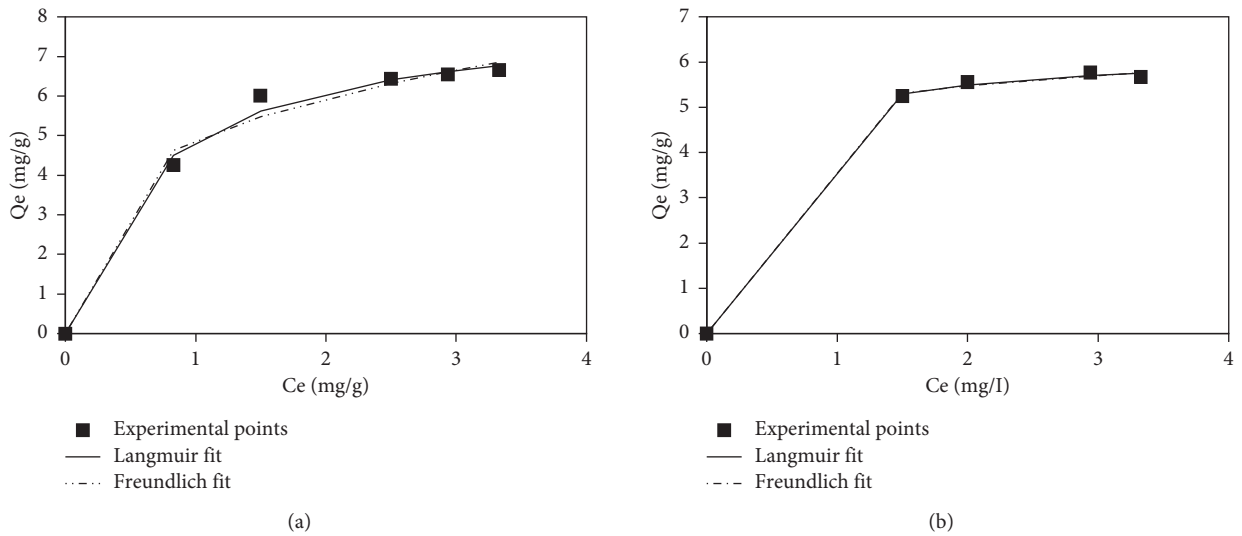

Figure 7: Continued.

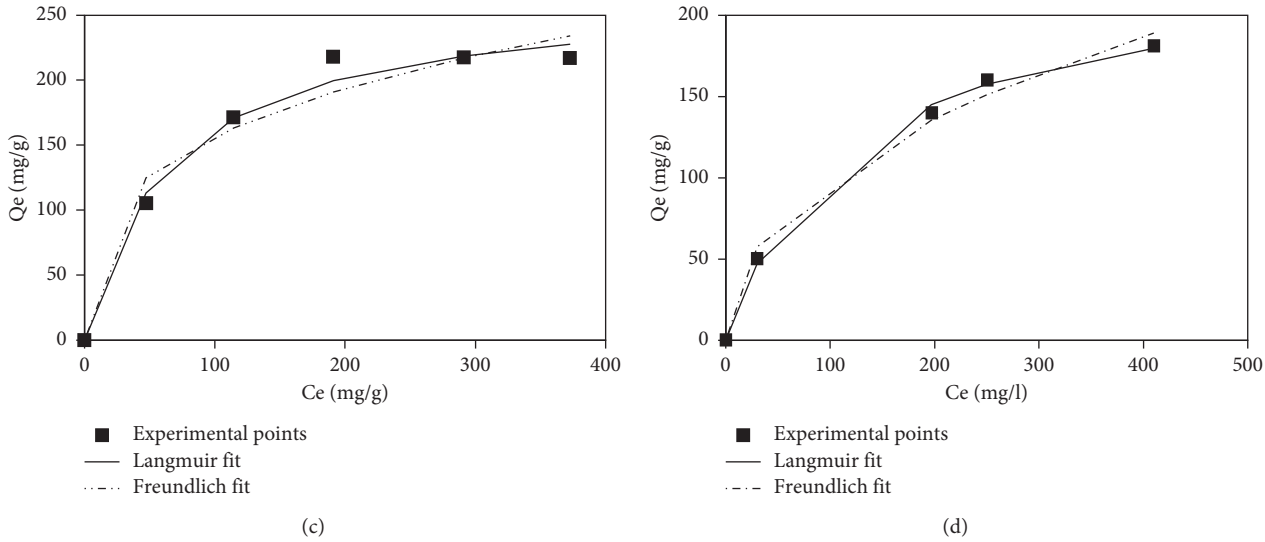

Figure 7: Isotherm sorption of BB onto A-NaOH (a), BB onto A-HCl (b), MB onto A-NaOH (c), and MB onto A-HCl (d).

constant related to the biosorption affinity. C_e is the equilibrium concentration.

(2) Freundlich Model. The Freundlich isotherm is an empirical model of heterogeneous surface sorption with nonuniform distribution of heat sorption and affinities [35]. The form of the Freundlich equation can be stated as follows:

$$Q_e = K_F C_e^{1/n}, \quad (9)$$

where K_F ($mg^{1-1/n}\ g^{-1}\ L^{1/n}$) and n are Freundlich constants. n is the heterogeneity factor related to biosorption affinity and K_F is related to the biosorption capacity.

If the values of n are in the range of 1–10, it can be considered that the biosorption process indicates a favorable and slightly difficult biosorption. However, the biosorption is very insignificant when n is lower than 1. Also, if the value of n is equal to unity, the biosorption is linear; if the value is below unity, it can be deduced that biosorption process is chemical, and if the value is above unity, adsorption is a favorable physical process.

Biosorption parameters of Langmuir and Freundlich models of BB and MB onto A-HCl and A-NaOH are grouped in Table 3. From this table, the Langmuir model indicates higher values of correlation coefficients in the biosorption of the both dyes onto A-NaOH and A-HCl. In addition, the Langmuir model has higher r^2 values than the Freundlich isotherm model. These results indicate that the biosorption of BB and MB is more fitted to Langmuir model.

In fact, it could be seen that the biosorption onto A-NaOH is more efficient than that one onto A- HCl. This result could be due to the greater surface area of A-NaOH, where the NaOH increases the dissociated groups and creates well-developed pores on the surface of the material. It appears that the large specific surfaces have a greater biosorption capacity unlike the lower surfaces under the same conditions of experience. On the other hand, the biosorption of MB is greater than that of BB onto the both biosorbents, and this may be due to the molecular weight of MB that was lower when compared to the BB molecule. Also, BB dye has a large structure with aromatic cycles and contains SO_3^- groups which are special orthogonal groups in 3 dimensions; it is a highly reactive substance. It could be deduced that the BB dye

Table 3: Parameters relating to Langmuir and Freundlich isotherm equations.

		Langmuir			Freundlich		
		R^2	q_{max} (mg/g)	K (L/mg)	R^2	n	K
BB	A-NaOH	0.993	8.13	1.48	0.985	3.54	4.88
	A-HCl	0.999	6.19	3.89	0.998	9.84	5.10
MB	A-NaOH	0.986	267.04	0.02	0.961	3.27	38.43
	A-HCl	0.998	230.65	0.01	0.990	2.19	12.20

Table 4: Comparison of maximum biosorption capacity of A-NaOH and A-HCl for MB with corresponding low-cost biosorbents.

Biosorbent	q (mg/g) MB	References
Diplotaxis harra	185.59	[18]
Glebionis Coronaria L.	258.76	[18]
Carica papaya wood	32.25	[36]
M. Bacillus subtilis	59 ± 0.6	[37]
Caulerpa racemosa var. cylindracea	5.23	[38]
Living biomass	1.17	[39]
Acacia fumosa seed shell	1.85	[40]
Coconut coir dust	29.50	[41]
Cereal chaff	20.30	[42]
Acacia sawdust-NaOH	267.04	This study
Acacia sawdust-HCl	230.65	This study

Table 5: Results of the physicochemical characterization of the industrial effluent.

Parameters		T (°C)	pH	Conductivity (μS. cm^{-1})	COD (mg/L)	BOD_5 (mg/L)	NTK (mg/L)	P (mg/L)	MES (mg/L)
Final discharge	Ech 1	27.5	8.99	188	662.4	338	140.1	2.4152	2444
	Ech 2	27.1	9.03	182	653.6	349	112.08	—	1948
	Ech 3	26.8	9.01	189	659.1	322	127.3	—	2192
	Average	27.13	9.01	186	658.36	336.3	126.49	2.4152	2194.6@
Discharged Water Standards (Bulletin Officiel., 2013)	30	5.5–8.5	2700	120	40	40	2	30	

has a complicated structure that may obstruct its sorption.

The maximum Langmuir biosorption capacities were 8.13, 6.19 mg/g for BB and 267.04, 230.65 mg/g in the case of MB, respectively, for A-NaOH and A-HCl. The biosorption capacities for MB dye were compared to the previous records of various low-cost biosorbents as summarized in Table 4. It can be observed that the experimental data of the present study were found to be higher than those of the most corresponding biosorbents in the literature. The higher biosorption capacities this study can be due to the nature of functional groups present on the surface of both biosorbents.

3.3. Biosorption Treatment of the Industrial Effluent

3.3.1. Physicochemical Characterization of the Studying Effluent before Biosorption. The average values of physicochemical characterization results of the studying effluent are listed in Table 5. These results were compared with those of the limit values relating to the quality of wastewater discharge standards into surface water [42]. It could be seen that average values of samples present a temperature and a conductivity less than the standard values; however, they have higher values for the other parameters.

However, the results of the metallic characterization of the studying effluents are listed in Table 6. The analysis of these results reveals a high concentration of chromium 0.908 mg/L. It could be seen that it was the origin of the toxicity of different dyes used in the treatment of jean, and therefore, its value was higher to standards of recommended rejects [42].

3.3.2. Biosorption Studies

(1) Kinetic Sorption. The result of the kinetic sorption of the polluted charge is shown in Figure 8. A strong increase in the percentage removal at the beginning of the sorption process has been seen. The rapid step is probably due to the availability of active sites on the both biosorbents. After that, the biosorption becomes less efficient when the curve shows a stagnation sign of stabilization and saturation of materials when the equilibrium is achieved. The times required to reach equilibrium are respectively 30 minutes of stirring for biosorption onto A-NaOH and about 45 minutes for A-HCl. The decolorization rates of the industrial effluent are 77% and 98% for A-HCl and A-NaOH, respectively.

Table 6: Results of the metallic characterization.

Heavy metals (mg/L)	Cd	Cr	Cu	Ni	Zn
Reject final	0.0482	*0.908*	<0.01	<0.01	0.3021
Discharged Water Standards	0.2	0.5	3	5	5

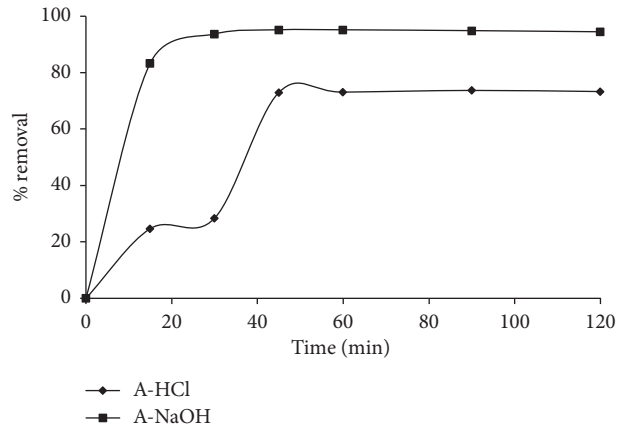

Figure 8: Adsorption kinetics of the industrial effluent on A-NaOH and A-HCl ($R = 1$g/l, $T = 25$°C).

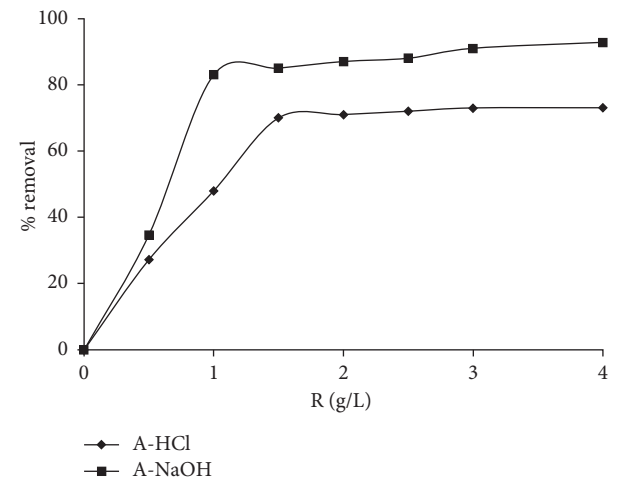

Figure 9: Effect of adsorbent dosage on the discoloration rate of the industrial effluent A-NaOH and A-HCl.

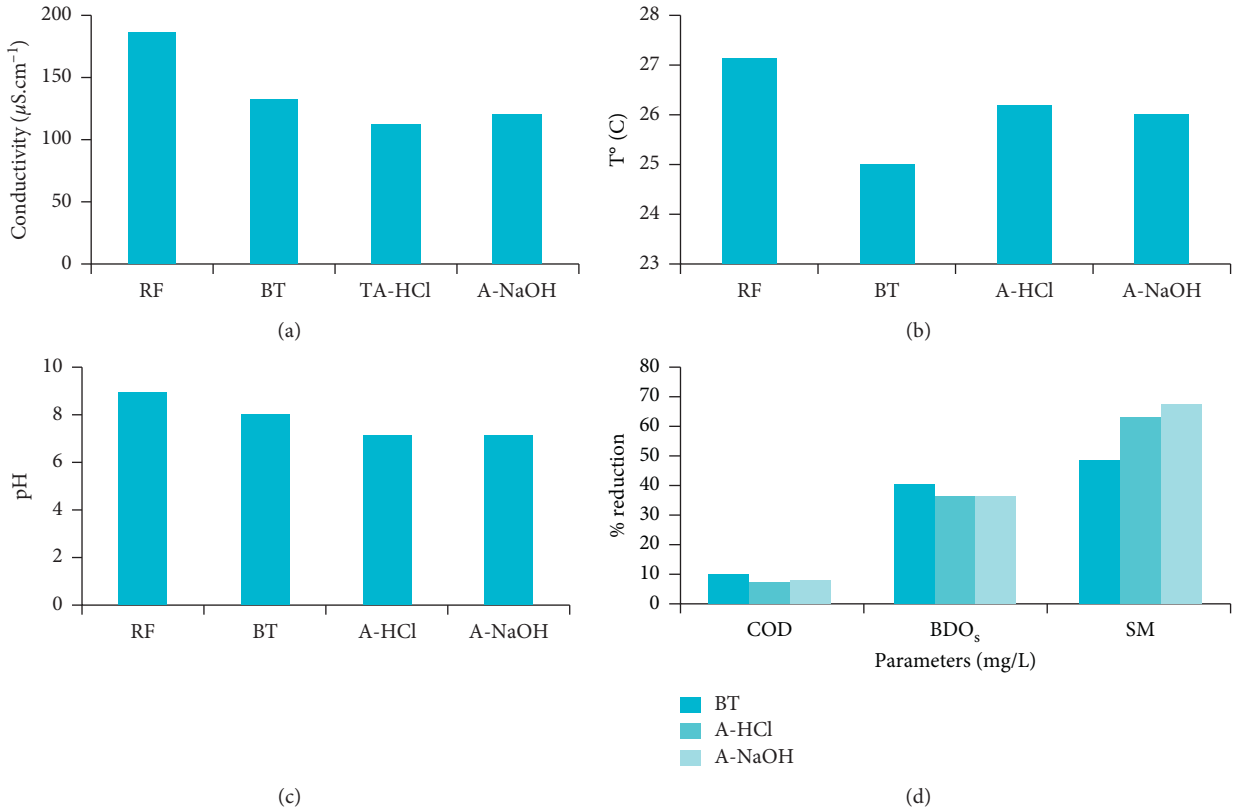

Figure 10: Characterization of the industrial effluent after treatment.

Therefore, Figure 8 indicates that the decolorization rate of the effluent onto A-NaOH is more significant than that sorbed onto A-HCl. This result suggests that the biosorbent treated by NaOH contains more active sites than that treated with HCl. Also, this higher sorption can be due to the large A-NaOH surface area which is directly related to the porosity of this adsorbent and the presence of many active sites on its surface.

(2) Effect of Biosorbent Dosage. The data obtained from experiments through variation mass of biosorbents are presented in Figure 9. The figure shows that the percentage removal of the polluted charge of the industrial effluent increases when the mass of biosorbents increases. This could be due to the increase in the total available surface and the number of active sites.

The percentage of discoloration of the industrial effluent increased from 27.2% to 73.05% and from 34.7% to 92.8% when the mass of biosorbents is increased from 0.5 to 4 g/L, respectively, for acacia sawdust treated with HCl or NaOH. The biosorption yield was almost stable when the mass ratios were greater than 1.5 g/L and 1 g/L for the A-HCl and A-NaOH biosorbents, respectively.

According to these curves, it can be concluded that the biosorption onto A-NaOH was greater than that one onto A-HCl. This result can be attributed to the point of zero charge and the large A-NaOH surface area.

3.3.3. Characterization of the Industrial Effluent after Biosorption Treatment. The results of the characterization of the industrial effluent after biosorption and biological treatment elaborated by the textile industry are given in Figure 10.

From this figure, it appears that the treatment of industrial effluent by the biosorption on chemically treated acacia sawdust or by biological treatment carried out by the industry itself remains insufficient. Therefore, the combination of the both treatments was recommended for better results since the biological treatment gives better results in terms of biological parameters (COD and BOD_5); however, the physicochemical treatment treats effectively the color, the MES, and the odor of the studied effluent.

4. Conclusion

In this work, chemically treated acacia sawdust was used as low-cost biosorbents for the removal of methylene blue and brilliant blue from aqueous solutions. This study investigated the optimal parameters for the removal of textile dyes using the both biosorbents derived from acacia sawdust A-HCl and A-NaOH. The ability of these materials was investigated using kinetic and equilibrium studies and the effect of dosage adsorbents. In fact, the biosorption of BB and MB increases with the increase of the biosorbent dosage with an optimum at 0.5 g/L. It was found that the sorption process was very rapid; the equilibrium time was obtained at 40 min for BB and 90 min for MB. The biosorption kinetic data were more suitable to the pseudo-first-order kinetic model. The equilibrium uptake of these dyes was increased by the increase of the initial concentration. The biosorption

equilibrium data of the brilliant blue and methylene blue dyes onto the both biosorbents were best fitted according to the Langmuir isotherm model. The biosorption capacities are 8.13 and 267.04 mg/g onto basic sawdust acacia and 6.19 and 230.76 mg/g onto acidic sawdust acacia, respectively, for BB and MB sorption. Under the experimental conditions, the A-NaOH gives more effective results than A-HCl, whereas raw sawdust acacia does not give satisfactory results since it relives a remarkable coloration in the solution.

For more enhanced adsorption results, a real final effluent of textile industry was treated. The kinetic sorption of this effluent was rapid with a mass ratio of 1 g/L with a higher removal of polluted charges through A-NaOH. However, the adsorption process combined with a biological treatment investigates a better result by studying physicochemical characteristics.

Data Availability

The characterization methods data and reagent materials and used biosorbents data used to support the findings of this study are included within the article. The water samples and their methods of analysis are those recommended by AFNOR and enacted by Rodier (J. Rodier, L'Analyse de l'eau, 9ième Edition. L'analyse de l'eau-9ème édition-Eaux naturelles, eaux résiduaires, eau de mer (2009)). The isotherm models data, kinetic models data, and maximum biosorption capacity of low-cost biosorbents data used to support the findings of this study have been deposited in the references. Previously reported (Discharged Water Standards (Bulletin Officiel., 2013)) data were used to support this study and are available at (Bulletin Officiel, Edition de traduction officielle, royaume du Maroc, N° 6202. (2013)). These prior studies (and datasets) are cited at relevant places within the text as references. The preparation and characterization of biosorbents data used to support the findings of this study are available from the corresponding author upon request.

Conflicts of Interest

The authors declare that they have no conflicts of interest.

Acknowledgments

The authors gratefully thank "Laboratoire d'ingénierie d'Electrochimie de Modélisation et d'Environnement", Faculty of Sciences Dhar EL Mahraz, Sidi Mohamed Ben Abdellah University, Fez, Morocco. Also, they specially thank the innovation unit of Sidi Mohamed Ben Abdellah University.

References

[1] A. Khatri, M. H. Peerzada, M. Mohsin, and M. White, "A review on developments in dyeing cotton fabrics with reactive dyes for reducing effluent pollution," *Journal of Cleaner Production*, vol. 87, pp. 50–57, 2015.

[2] B. Mu, W. Li, H. Xu, L. Xu, and Y. Yang, "Freeze-extrusion for controllable assembly of 3-dimensional ultra-fine and amorphous fibrous matrices: potential applications in sorption," *Journal of Materials Chemistry A*, vol. 6, no. 22, pp. 10320–10330, 2018.

[3] A. Ghaly, R. Ananthashankar, M. Alhattab, and V. Ramakrishnan, "Production, characterization and treatment of textile effluents: a critical review," *Journal of Chemical Engineering & Process Technology*, vol. 5, pp. 1–19, 2014.

[4] J. M. Rosa, A. M. F. Fileti, E. B. Tambourgi, and J. C. C. Santana, "Dyeing of cotton with reactive dyestuffs: the continuous reuse of textile wastewater effluent treated by ultraviolet/hydrogen peroxide homogeneous photocatalysis," *Journal of Cleaner Production*, vol. 90, pp. 60–65, 2015.

[5] A. A. Atia, A. M. Donia, and W. A. Al-Amrani, "Adsorption/desorption behavior of acid orange 10 on magnetic silica modified with amine groups," *Chemical Engineering Journal*, vol. 150, no. 1, pp. 55–62, 2009.

[6] F. Çolak, N. Atar, and A. Olgun, "Biosorption of acidic dyes from aqueous solution by Paenibacillus macerans: kinetic, thermodynamic and equilibrium studies," *Chemical Engineering Journal*, vol. 150, no. 1, pp. 122–130, 2009.

[7] E. S. Z. E. Ashtoukhy, "Removal of color and cod from aqueous solution containing dyes by electrocoagulation in a new cell," *Environmental Engineering and Management Journal*, vol. 13, no. 3, pp. 499–508, 2014.

[8] M. Sena and A. Hicks, "Life cycle assessment review of struvite precipitation in wastewater treatment," *Resources, Conservation and Recycling*, vol. 139, pp. 194–204, 2018.

[9] R. Lafi, L. Gzara, R. H. Lajimi, and A. Hafiane, "Treatment of textile wastewater by a hybrid ultrafiltration/electrodialysis process," *Chemical Engineering and Processing - Process Intensification*, vol. 132, pp. 105–113, 2018.

[10] Z. Kiayi, T. B. Lotfabad, A. Heidarinasab, and F. Shahcheraghi, "Microbial degradation of azo dye carmoisine in aqueous medium using *Saccharomyces cerevisiae* ATCC 9763," *Journal of Hazardous Materials*, vol. 373, pp. 608–619, 2019.

[11] N. Nippatla and L. Philip, "Electrocoagulation-floatation assisted pulsed power plasma technology for the complete mineralization of potentially toxic dyes and real textile wastewater," *Process Safety and Environmental Protection*, vol. 125, pp. 143–156, 2019.

[12] J. Li, Y. Li, Z. Xiong, G. Yao, and B. Lai, "The electrochemical advanced oxidation processes coupling of oxidants for organic pollutants degradation: a mini-review," *Chinese Chemical Letters*, vol. 30, no. 12, pp. 2139–2146, 2019.

[13] A. Giwa, A. Dindi, and J. Kujawa, "Membrane bioreactors and electrochemical processes for treatment of wastewaters containing heavy metal ions, organics, micropollutants and dyes: recent developments," *Journal of Hazardous Materials*, vol. 370, pp. 172–195, 2018.

[14] M. Qasim, M. Badrelzaman, N. N. Darwish, N. A. Darwish, and N. Hilal, "Reverse osmosis desalination: a state-of-the-art review," *Desalination*, vol. 459, pp. 59–104, 2019.

[15] W. Li, B. Mu, and Y. Yang, "Feasibility of industrial-scale treatment of dye wastewater via bio-adsorption technology," *Bioresource Technology*, vol. 277, pp. 157–170, 2019.

[16] V. Katheresan, J. Kansedo, and S. Y. Lau, "Efficiency of various recent wastewater dye removal methods: a review," *Journal of Environmental Chemical Engineering*, vol. 6, no. 4, pp. 4676–4697, 2018.

[17] K. G. Pavithra, P. Senthil Kumar, V. Jaikumar, and P. Sundar Rajan, "Removal of colorants from wastewater: a review on sources and treatment strategies," *Journal of Industrial and Engineering Chemistry*, vol. 75, pp. 1–19, 2019.

[18] H. Tounsadi, A. Khalidi, M. Abdennouri, and N. Barka, "Potential capability of natural biosorbents:Diplotaxis harraandGlebionis coronariaL. on the removal efficiency of dyes from aqueous solutions," *Desalination and Water Treatment*, vol. 57, no. 35, pp. 16633–16642, 2016.

[19] A. C. Khorasani and S. A. Shojaosadati, "Magnetic pectin-Chlorella vulgaris biosorbent for the adsorption of dyes," *Journal of Environmental Chemical Engineering*, vol. 7, pp. 103–062, 2019.

[20] A. P. D. Oliveira, A. N. Módenes, M. E. Bragião, C. L. Hinterholz, D. E. G. Trigueros, and I. G. de Bezerra, "Use of grape pomace as a biosorbent for the removal of the Brown KROM KGT dye," *Bioresource Technology Reports*, vol. 2, pp. 92–99, 2018.

[21] S. Singh, N. Parveen, and H. Gupta, "Adsorptive decontamination of rhodamine-B from water using banana peel powder: a biosorbent," *Environmental Technology & Innovation*, vol. 12, pp. 189–195, 2018.

[22] D. C. C. de Silva and J. M. T. A. da Pietrobelli, "Residual biomass of chia seeds (Salvia hispanica) oil extraction as low cost and eco-friendly biosorbent for effective reactive yellow B2R textile dye removal: characterization, kinetic, thermodynamic and isotherm studies," *Journal of Environmental Chemical Engineering*, vol. 7, p. 103008, 2019.

[23] C. Li, X. Wang, D. Meng, and L. Zhou, "Facile synthesis of low-cost magnetic biosorbent from peach gum polysaccharide for selective and efficient removal of cationic dyes," *International Journal of Biological Macromolecules*, vol. 107, pp. 1871–1878, 2017.

[24] G. B. Kankılıc, A. Ü. Metinb, and I. Tüzüna, "Phragmites australis: an alternative biosorbent for basic dye removal," *Ecological Engineering*, vol. 86, pp. 85–94, 2016.

[25] A. Iqbal, S. Mun-Yee, M. N. N. Asshifa, A. R. M. Nur Asshifab, A. R. M. Yahya, and F. Adam, "*Pseudomonas aeruginosa* USM-AR2/SiO2 biosorbent for the adsorption of methylene blue," *Journal of Environmental Chemical Engineering*, vol. 6, no. 4, pp. 4908–4916, 2018.

[26] Y. A. R. Lebron, V. R. Moreira, and L. V. S. Santos, "Studies on dye biosorption enhancement by chemically modified Fucus vesiculosus, Spirulina maxima and Chlorella pyrenoidosa algae," *Journal of Cleaner Production*, vol. 240, p. 118197, 2019.

[27] J. S. Noh and J. A. Schwarz, "Estimation of the point of zero charge of simple oxides by mass titration," *Journal of Colloid and Interface Science*, vol. 130, no. 1, pp. 157–164, 1989.

[28] J. C. Santamarina, K. A. Klein, Y. H. Wang, and E. Prencke, "Specific surface: determination and relevance," *Canadian Geotechnical Journal*, vol. 39, no. 1, pp. 233–241, 2002.

[29] W. Zhang, H. Tao, B. Zhang, J. Ren, G. Lu, and Y. Wang, "One-pot synthesis of carbonaceous monolith with surface sulfonic groups and its carbonization/activation," *Carbon*, vol. 49, no. 6, pp. 1811–1820, 2011.

[30] J. Rodier, *L'analyse de l'eau - 9ème édition - Eaux naturelles, eaux résiduaires, eau de mer*, Dunod, Paris, France, 9 edition, 2009.

[31] A. Alemdar and M. Sain, "Isolation and characterization of nanofibers from agricultural residues - wheat straw and soy hulls," *Bioresource Technology*, vol. 99, no. 6, pp. 1664–1671, 2008.

[32] S. Lagergren, "About the theorie of so-called adsorption of soluble substance Seven Vetenskapsakad," *HandBand*, vol. 24, pp. 1–39, 1898.

[33] Y. S. Ho and G. Mckay, "The kinetics of sorption of basic dyes from aqueous solution by sphagnum moss peat," *The Canadian Journal of Chemical Engineering*, vol. 76, no. 4, pp. 822–827, 1998.

[34] I. Langmuir, "The constitution and fundamental properties of solids and liquids. Part I. Solids," *Journal of the American Chemical Society*, vol. 38, no. 11, pp. 2221–2295, 1916.

[35] H. Freundlich and W. Heller, "The Adsorption ofcis- andtrans-Azobenzene," *Journal of the American Chemical Society*, vol. 61, no. 8, pp. 2228–2230, 1939.

[36] R. S, S. Lata, and B. P, "Biosorption characteristics of methylene blue and malachite green from simulated wastewater onto Carica papaya wood biosorbent," *Surfaces and Interfaces*, vol. 10, pp. 197–215, 2018.

[37] B. Tural, E. Ertaş, B. Enez, S. A. Fincan, and S. Tural, "Preparation and characterization of a novel magnetic biosorbent functionalized with biomass of Bacillus Subtilis : kinetic and isotherm studies of biosorption processes in the removal of Methylene Blue," *Journal of Environmental Chemical Engineering*, vol. 5, no. 5, pp. 4795–4802, 2017.

[38] U. J. Etim, S. A. Umoren, and U. M. Eduok, "Coconut coir dust as a low cost adsorbent for the removal of cationic dye from aqueous solution," *Journal of Saudi Chemical Society*, vol. 9, pp. 12–18, 2012.

[39] Y. Fu and T. Viraraghavan, "Removal of a dye from an aqueous solution by the fungus Aspergillus Niger," *Water Quality Research Journal*, vol. 35, no. 1, pp. 95–112, 2000.

[40] M. Kumar and R. Tamilarasan, "Modeling studies for the removal of methylene blue from aqueous solution using Acacia fumosa seed shell activated carbon," *Journal of Environmental Chemical Engineering*, vol. 1, no. 4, pp. 1108–1116, 2013.

[41] H. Runping, W. Yuanfeng, H. Pan, S. Jie, Y. Jian, and L. Yongsen, "Removal of methylene blue from aqueous solution by chaff in batch mode," *Journal of Hazardous Materials*, vol. 137, pp. 550–557, 2006.

[42] Bulletin Officiel, Edition de traduction officielle, royaume du Maroc, N° 6202. (2013).